Protein Science (1997), *6*:1009–1015. Cambridge University Press. Printed in the USA.

Three-dimensional structures of glycolate oxidase with bound active-site inhibitors

KAJ STENBERG AND YLVA LINDQVIST

Department of Medical Biochemistry and Biophysics, Karolinska Institute, Doktorsringen 4, S17177 Stockholm, Sweden

(RECEIVED January 6, 1997; ACCEPTED February 24, 1997)

Abstract

A key step in plant photorespiration, the oxidation of glycolate to glyoxylate, is carried out by the peroxisomal flavoprotein glycolate oxidase (EC 1.1.3.15). The three-dimensional structure of this α/β barrel protein has been refined to 2 Å resolution (Lindqvist Y. 1989. *J Mol Biol 209*:151–166). FMN dependent glycolate oxidase is a member of the family of α-hydroxy acid oxidases. Here we describe the crystallization and structure determination of two inhibitor complexes of the enzyme, TKP (3-Decyl-2,5-dioxo-4-hydroxy-3-pyrroline) and TACA (4-Carboxy-5-(1-pentyl)hexylsulfanyl-1,2,3-triazole). The structure of the TACA complex has been refined to 2.6 Å resolution and the TKP complex, solved with molecular replacement, to 2.2 Å resolution. The R_{free} for the TACA and TKP complexes are 24.2 and 25.1%, respectively. The overall structures are very similar to the unliganded holoenzyme, but a closer examination of the active site reveals differences in the positioning of the flavin isoalloxazine ring and a displaced flexible loop in the TKP complex. The two inhibitors differ in binding mode and hydrophobic interactions, and these differences are reflected by the very different K_i values for the inhibitors, 16 nM for TACA and 4.8 μM for TKP. Implications of the structures of these enzyme-inhibitor complexes for the model for substrate binding and catalysis proposed from the holo-enzyme structure are discussed.

Keywords: drug design; flavin enzyme; glycolate oxidase; inhibitor binding; molecular replacement; protein crystallography

Glycolate oxidase (EC 1.1.3.15, GOX) is a FMN-dependent α-hydroxy acid-oxidizing protein. In plants, the enzyme is located in the peroxisomes and performs a key step in photorespiration, the oxidation of glycolate to glyoxylate. In animals, the enzyme is located in the liver peroxisomes and is involved in oxalate production. The reaction catalyzed by the enzyme can be divided into two half-reactions. In the first half-reaction glycolate is oxidized by the flavin, and in the second part of the reaction, FMN is reoxidized by oxygen and hydrogen peroxide is formed (Macheroux et al., 1991).

The three-dimensional structure for GOX from spinach with bound FMN has been determined to 2 Å resolution (Lindqvist, 1989). The enzyme belongs to the class of eight stranded α/β-barrels, the most common structural motif found so far, with over 45 known examples. The known α/β-barrel folds do not share any recognizable sequence identity fingerprints, but do show extensive structural similarity.

Reprint requests to: Ylva Lindqvist, Department of Medical Biochemistry and Biophysics, Karolinska Institute, Doktorsringen 4, S17177 Stockholm, Sweden; e-mail: ylva@alfa.mbb.ki.se.

Abbreviations: JF5969, A mixture of Symperonic NPE1800 (ICI surfactants, UK) (33.3 g/L), TWEEN 85 (20 g/L), in cyclohexanone; TACA, 4-Carboxy-5-(1-pentyl)hexylsulfanyl-1,2,3-triazole; TKP, 3-Decyl-2,5-dioxo-4-hydroxy-3-pyrroline.

However, a significant proportion of the residues in GOX are highly conserved in several other FMN-dependent α-hydroxy acid-oxidizing enzymes. These proteins include (sequence identity % to GOX in brackets, values from Lê & Lederer, 1991) flavocytochrome b_2 (37.2) from *Saccharomyces cerevisiae* and *Hansenula anomala* (41.1), lactate oxidase (31.7) from *Mycobacterium smegmatis*, mandelate oxidase (33.4) from *Pseudomonas putida*, and α-hydroxy-acid oxidase (45.0) from the rat. The three-dimensional structure of the FMN-binding domain of yeast flavocytochrome b_2 has been shown to be highly similar to that of spinach GOX (Lindqvist et al., 1991); 311 structurally equivalent Cα-atoms in GOX and the FMN-binding domain of flavocytochrome b_2 show a root-mean-square deviation (RMSD) of 0.93 Å. It is likely that other proteins in this family also have a very similar structure beyond the α/β-barrel fold.

A model describing substrate binding based on the 3D structure of spinach holo-GOX has been put forward (Lindqvist & Brändén, 1989). The active site is formed by the loops at the C-terminal end of the β-strands in the barrel, as is usually found in α/β-barrel proteins. Additional helices besides the α/β-fold are located at the C-terminal end of the β-strands and form a "lid," partly shielding the active site. The cofactor FMN is deeply buried in the barrel, with only the N5 atom exposed to the solvent from the substrate cavity. From the structure, the charged residues Arg 257 and Arg 164 were proposed to bind the carboxyl-group of the substrate,

with participation of Tyr 24 (Lindqvist & Brändén, 1989). Site-directed mutagenesis studies have shown that the two tyrosines, Tyr 24 and Tyr 129, are involved in substrate binding and stabilization of the transition state, respectively (Macheroux et al., 1993; Stenberg et al., 1995) and that Trp 108 is involved in substrate specificity (Stenberg et al., 1995).

To date, it has not been possible to obtain structural information for any complex of GOX with bound substrates, products, or inhibitors. In plants, the inhibition of GOX has been studied in the search of a herbicide. In humans, inhibition of GOX has been considered as a possibility in treatment of some oxalate-mediated disorders, like hyperoxaluria and renal lithiasis (Rooney et al., 1983; Williams et al., 1983; Jayanthi et al., 1994), and inhibitor studies have been carried out using both mammalian and plant GOX (Fendrich & Ghisla, 1982; Rooney et al., 1983). High-sequence identity (45%) between the spinach enzyme and its isozyme, long-chain α-hydroxy acid oxidase from rat (Lê & Lederer, 1991) indicates that results from the spinach enzyme can to some extent be extrapolated to mammals. A database search revealed a human cDNA sequence, which when translated, produced a 128 amino acid long peptide (GenBank Database accession number T64673). This fragment shows a 50% identity to the N-terminal part of spinach GOX, with the active site residues Tyr 24 and Trp 108 conserved. This finding is in favor of the assumption that FMN-dependent α-hydroxy acid oxidases are very similar over species boundaries.

Studies of inhibitors bound to GOX might also provide some information about substrate binding and the catalytic mechanism. Here we report the structures of two enzyme-inhibitor complexes of spinach GOX.

Results

Crystallization

Yellow crystals of holo GOX in complex with TACA (formula in Fig. 1) grow in one week. The crystals are isomorphous to crystals of the holoenzyme and belong to the space group I422 ($a = b =$ 148.1 Å, $c =$ 135.1 Å) with one molecule in the asymmetric unit, and diffract to 2.6 Å. With TKP (formula in Fig. 1) brownish crystals that diffract to 2.2 Å can be obtained. The crystals belong to the space group I4 ($a = b =$ 95.4 Å, $c =$ 93.5 Å), with one molecule in the asymmetric unit.

Overall structures of the complexes

The structures for the two inhibitor complexes were solved and refined to 2.6 Å resolution for TACA and 2.2 Å for TKP. The free-R factor is 25.1 for the complex with TACA and 24.2 for the TKP–complex. The stereochemistry of the protein chain is good in both complexes; the RMSD from ideality for bond lengths in the TACA and TKP complexes are 0.007 Å and RMSD for angles are 1.38° and 1.37°, respectively. Details of the refinement and the protein models are summarized in Table 1.

A Ramachandran plot of the TACA complex shows that 90.6% of the residues are found in the most favored regions and 0.6% (three residues) in disallowed regions. The corresponding figures for the TKP–complex are 92.4 and 0.3% (two residues). One residue with disallowed phi-psi angles in the TACA–complex is Glu 30, which is located in a turn between two α-helices. In the holoenzyme structure, refined at 2 Å resolution, this residue also adopts a disallowed conformation (Lindqvist, 1989). Other disallowed conformations are adopted by residues 200 and 188, which are adjacent to the gap present in the model and show very weak density. The disallowed conformations in the TKP–complex are residues Glu 30 and Tyr 202; the latter has a very weak electron density and is probably rather flexible. It is of interest to note that Thr 78, which in the holoenzyme structure adopts a disallowed conformation, is in a more favorable conformation in both complex structures.

The overall structures are very similar to the holoenzyme structure with RMSD 0.25 Å for the TACA complex and 0.71 Å for TKP. The difference between the TKP complex and the holoenzyme is not evenly spread, but is mainly found in the region between residues 155 and 180 (Fig. 2). Furthermore, for the TKP complex there is very weak electron density in the region between residues 160 and 170, indicating a less ordered structure. The electron density for residues 162–167 could not be interpreted, and these residues were omitted from the model. The gap in electron

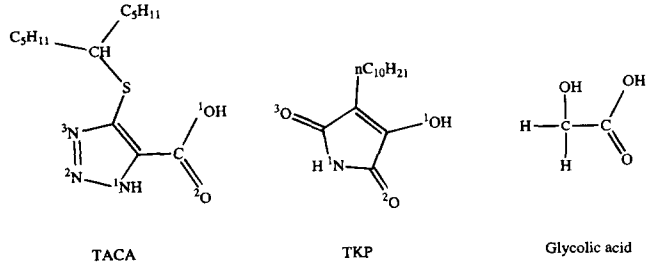

Fig. 1. The molecular formulas of the inhibitors TACA, TKP, and the substrate glycolate.

Table 1. *Data collection and refinement statistics*

	TACA	TKP
Data		
Space group	I422	I4
Cell axes (Å)		
$a = b$	148.1	95.4
c	136.5	93.5
Resolution (Å)	2.6	2.2
No reflections	48,698	237,398
Unique	20,291	21,308
Completeness (%)	87.1 (100–2.6Å)	99.8 (100–2.2Å)
Highest resolution shell	74.4 (2.68–2.6Å)	99.9 (2.25–2.2Å)
Redundancy	2.4	11.1
R_{merge}	8.5	9.4
Refinement		
No. reflections	20,005 (8–2.6Å)	21,198 (8–2.2Å)
R	18.0	19.4
R_{free} (8%)	24.2	25.1
Number of protein non-H atoms	2,721	2,683
Number of water and ligand Non-H atoms	318	85
Stereochemistry		
RMSD		
Bonds (Å)	0.007	0.007
Angles (°)	1.38	1.37
Average B (Å^2)	23.2	27.6
RMS B (Å^2)		
Cross bonds[a]	1.36	1.35
Cross angles[a]	1.92	1.93

[a]Calculated using a program by Guoguang Lu (unpublished).

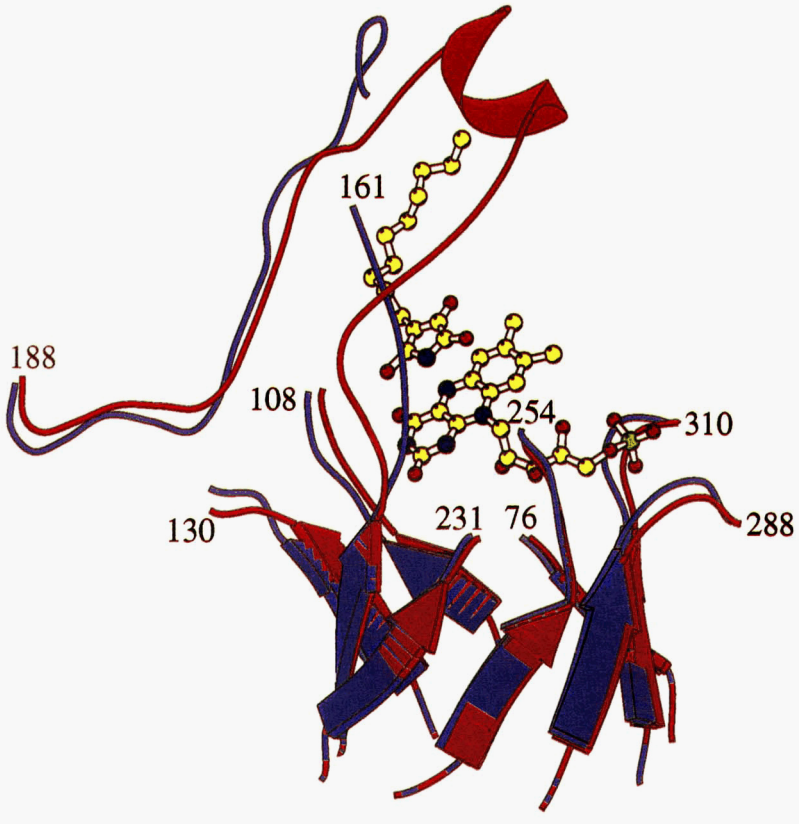

Fig. 2. Superimposition of the holoenzyme (red) and the TKP complex (blue). For purposes of clarity, only the β-strands of the barrel and a region that had to be rebuilt in the complex are shown. The inhibitor and FMN are shown as ball-and-stick models. The figure was produced using MOLSCRIPT (Kraulis, 1991).

density between amino acid residues 188 and 198 observed for the native structure is found in both of the enzyme complexes, and electron density for residues 198 and 202 is weak. In both inhibitor complexes the isoalloxazine ring of FMN has a changed position compared to the holoenzyme and has moved about 30° toward the *re*-side corresponding to a distance of 1.7 Å for the N3-atom (Fig. 5a), with a corresponding change in the positions for the side chains of His 254. The ribityl side chains of FMN are affected only slightly. The movement of the isoalloxazine ring closes a cavity on the *re*-face of the flavin ring. This cavity, in the holoenzyme structure occupied by a water molecule, has been proposed to play a central role in the oxidative half-reaction of the enzyme (Lindqvist & Brändén, 1989).

TACA complex

The inhibitor is bound in the postulated active site at the C-terminal end of the β-strands of the barrel. TACA is well ordered in the active site and the branched hydrocarbon tail can be followed to its full length, indicating limited flexibility (Fig. 3). Interactions are formed between two of the nitrogens in the head group and the side chains of Tyr 129 and His 254, respectively. Close contacts, indicative of hydrogen bonds, are observed between the carboxyl group of the inhibitor and the side chains of Arg 257 and Tyr 24, and also for the side chain of Arg 164. One of the tails of TACA binds into a hydrophobic pocket formed by the side chains of Trp 108, Ile 207, Tyr 131, and Tyr 129. This pocket has been created by a movement of the side chain of Trp 108 away from the catalytic site. The other tail of TACA forms hydrophobic interactions to the phenyl ring of Phe 172 and the side chain of Leu 161.

Some additional differences to the holoenzyme can be observed besides the change in position of the isoalloxazine ring and the side chain of His 254. The side chains of tyrosines 24 and 129 have moved slightly to be able to form the hydrogen bonds. The side chain of Arg 164 is reoriented toward the inhibitor. Distances between the side chain nitrogens of the arginine and the inhibitor carboxyl oxygens are 3.2 and 3.0 Å. The tilt of the isoalloxazine ring toward its *re*-face forces a slight movement of Thr 78, which adopts a more favorable conformation than found for the holoenzyme. No other significant changes in structure can be observed at this resolution.

TKP complex

The electron density map is clear for the head part, but less ordered for the alkyl tail and the inhibitor could easily be built into the active site of GOX (Fig. 4). The exact bonding pattern is slightly different from that of TACA. Hydrogen bonds are formed between the oxygen atoms in the head group of the inhibitor to the side chains of residues Trp 108, Tyr 129, Tyr 24, Arg 257, and from the nitrogen atom of the inhibitor to that of histidine 254 (Fig. 5b).

Compared to the holoenzyme, the side chains of tyrosines 24 and 129 have moved to form the hydrogen bonds to the inhibitor. The side chain of Trp 108 has shifted its position to bring the

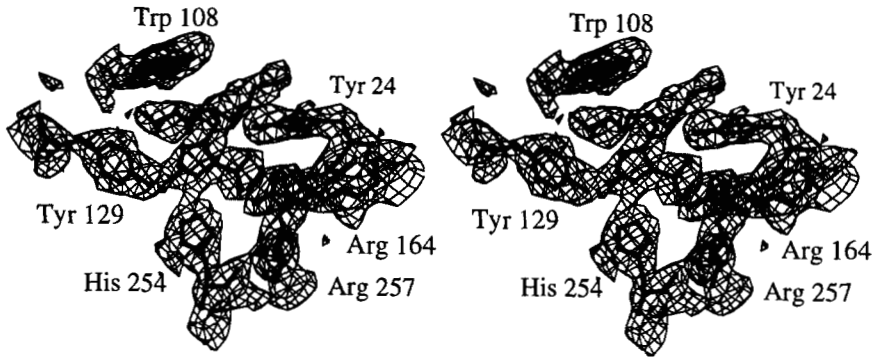

Fig. 3. Part of the electron density map for the complex of GOX-TACA. The $2F_o - F_c$ electron density map is contoured at 1.1σ level. The figure was made using the graphics program O (Jones et al., 1991).

nitrogen atom within hydrogen bonding distance to an oxygen on the inhibitor. The long alkyl tail of the inhibitor seems to be rather flexible, judging from the rather poor quality of the electron density for this part (Fig. 4), but is to some extent stabilized by the well-defined side chains of Met 80 and Phe 172. These side chains have moved considerably compared to the holoenzyme and the TACA complex. As modeled, the tail seems to be largely responsible for the observed conformational change between residues 155 and 180, a region that had to be rebuilt in this structure (Fig. 2). In the holoenzyme, this region consists of two loops, intercepted by a short α-helix between residues 165 and 169. In the inhibitor complex, the region is well defined, except around residues 162–167, which are invisible in the electron density.

The tilt of the isoalloxazine ring and the hydrophobic interaction between the inhibitor tail and the side chain of Met 80 causes a conformational change between residues 78 and 80 (Fig. 5a). The electron density for this region is very clear, indicating a very specific conformational change of the residues, including the main chain backbone.

Discussion

The two inhibitors bind with their rings stacked to the isoalloxazine ring of FMN, and superimposition of the two inhibitors (Fig. 5b) reveals a good agreement between the positioning of some of the polar atoms in the inhibitor head groups. The hydrogen bonding patterns are also very similar. One notable exception is Trp 108, which is not interacting with TACA, but forms a hydrogen bond with TKP. The residue Trp 108 has been shown to have a vital role in determining substrate specificity, probably via size exclusion (Stenberg et al., 1995). The inhibitors adopt a different strategy toward this tryptophan. TACA, being the bulkier and more rigid structure, pushes the aromatic ring away with its carbon double tail. TKP, being slightly smaller and with a more flexible tail forms a hydrogen bond toward one edge of the ring.

The long alkyl tail of TKP is forcing a positional change of the loops flanking the α-helix between residues 165–169 (Fig. 2). Destabilization of the region between residues 161 and 168 results in disorder, as indicated by weak or absent electron density for this part. The destabilized region contains several residues that are conserved between GOX and flavocytochrome b_2 (Lindqvist et al., 1991); three of the six missing residues are conserved, and particularly the side chain of Arg 164 is participating in forming the active site pocket. TKP, therefore, has a somewhat different binding environment than TACA. In the holoenzyme the side chains of residues Arg 164 and Arg 257 form a positive surface. The carboxyl oxygens of TACA are positioned 2.9–3.3 Å from these charges, forming strong ionic interactions. TKP is also negatively charged, pK_a = 5.3 (Rooney et al., 1983), but the oxygens in TKP are further apart, with the negative charge mainly localized to the oxygen labeled O1 (Fig. 1), and might not be able to match the positive charge in the pocket as well. This results in a conformational change of the side chain of Arg 164 and its immediate surroundings, thus avoiding burial of a positive charge. The ob-

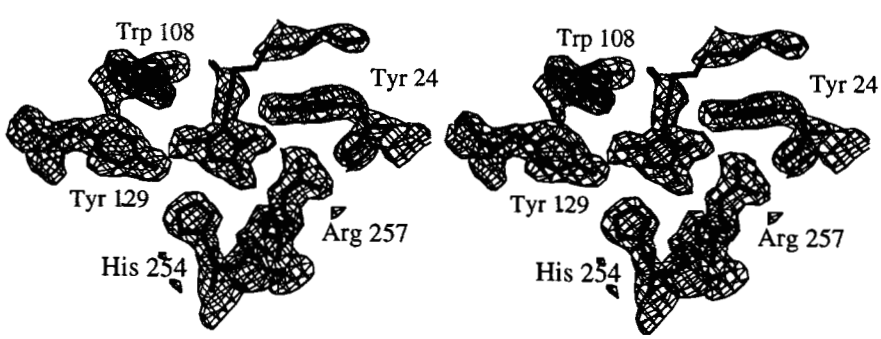

Fig. 4. Electron density in the active site of the complex of GOX and TKP. The $2F_o - F_c$ electron density map is contoured at 1.1σ level. The figure was made using the graphics program O (Jones et al., 1991).

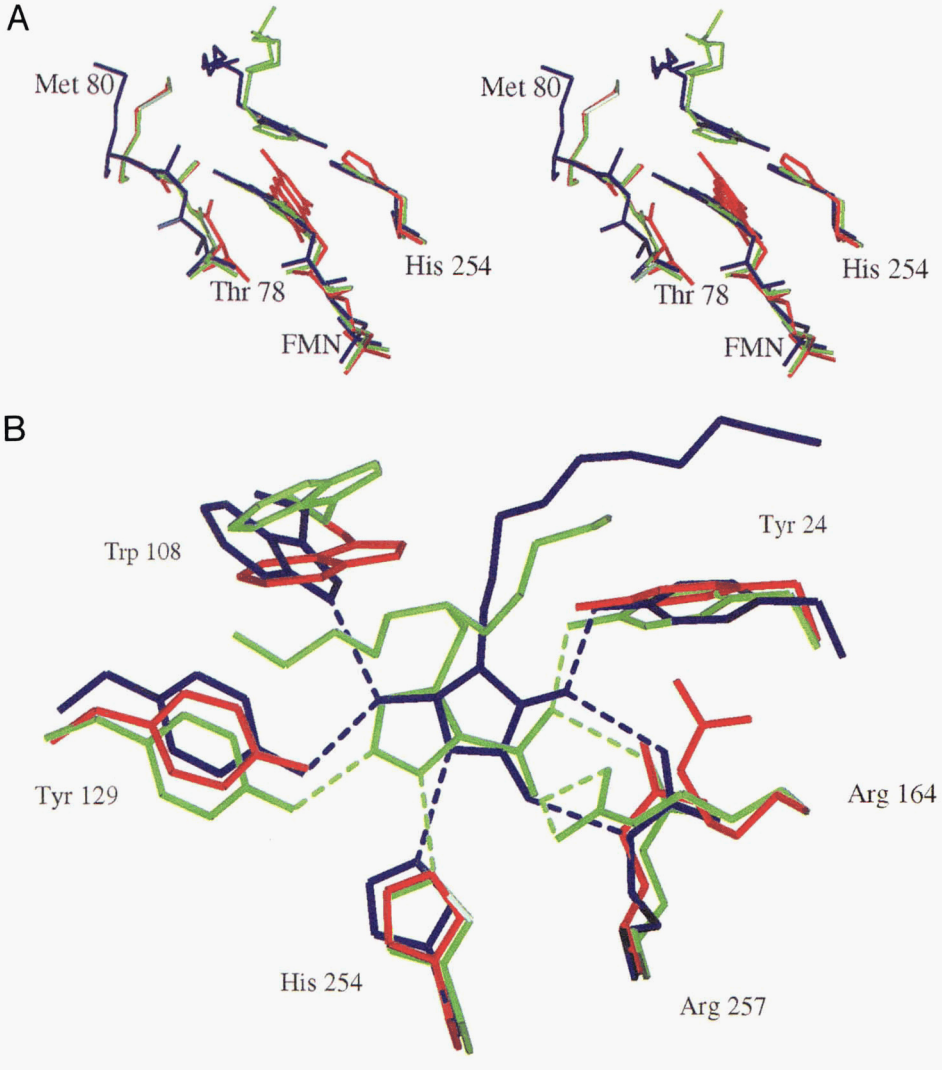

Fig. 5. A: Illustration of the positional shift of the flavin isoalloxazine ring in the inhibitor complexes. The structures of the holoenzyme (red), the TACA complex (green), and the TKP complex (blue) are superimposed. **B:** The hydrogen bonding pattern of the inhibitors at the active site of GOX. The holoenzyme is colored red, the TACA complex green, and the TKP complex blue. Distances less than 3.2 Å from the inhibitors are marked with dashed lines.

served large difference in K_i for the inhibitors, 16 nM for TACA and 4.8 μM for TKP (R. Viner et al., in prep.) can also be rationalized as an effect of the much better stabilization of the forked tail of TACA, with more favorable hydrophobic interactions. Even though TKP forms an extra hydrogen bond to Trp 108, this is obviously not enough to compensate for the stronger electrostatic interactions and better hydrophobic contacts of TACA.

One striking feature of the α-hydroxy acid oxidase enzyme family is the conservation of the active site residues around the flavin binding site. Six amino acids are conserved within the family, except for long-chain α-hydroxy-acid oxidase where the residue corresponding to Tyr 24 in GOX is replaced with a phenylalanine (Lê & Lederer, 1991). Mutational analysis of GOX and several of the related enzymes has proposed a role for many of the conserved residues (for a review, see Lederer et al., 1996). The active site of the GOX holoenzyme contains three water molecules, which, combined with the narrow substrate channel and pocket, have been used as a starting point for modeling the binding of substrate (Lindqvist & Brändén, 1989). In the proposed model the carboxyl part of glycolate is bound to Arg 257 and Tyr 24, while the hydroxyl group is bound to Tyr 129 (Fig. 6). Site-directed mutagenesis studies of GOX have confirmed the importance of Tyr 24 for substrate binding (Stenberg et al., 1995), whereas the main role of Tyr 129 seems to be in stabilizing the transition state, because the tyr $\rightarrow$ phe mutation showed little influence on binding affinity (Macheroux et al., 1993). Arg 257 has been studied in flavocytochrome b_2, where replacing the homologous Arg 376 with lysine completely abolishes activity (Reid et al., 1988).

A histidine residue (His 254 in GOX) is supposed to be responsible for abstracting a proton from the substrate in the oxidative half-reaction (Urban & Lederer, 1985). After the abstraction of a substrate proton, two possibilities exist for the reaction to proceed. In the most favored model the α-proton has been abstracted and a carbanion is formed before the transfer of electrons to FMN (Fig. 6). It has not, however, been ruled out that the proton initially abstracted is the hydroxyl proton and that the α-hydrogen is trans-

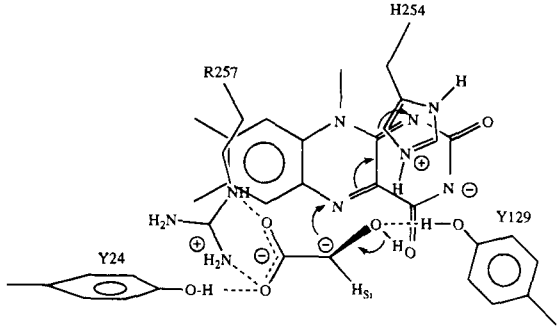

Fig. 6. Schematic picture of the active site of GOX after proton abstraction from glycolate.

ferred from the substrate via hydride transfer to the isoalloxazine ring (Ghisla & Massey, 1989).

Examining the inhibitor complexes gives support to the model of the enzyme–substrate complex. TACA has a carboxyl group that is likely to mimic that of glycolic acid (Fig. 1). In the model, however, the substrate makes a hydrogen bond to Tyr 129. This residue has been shown to participate mainly in transition state stabilization, and not in initial binding of the substrate (Macheroux et al., 1993). Both inhibitor complexes also show a hydrogen bond to Tyr 129, as well as to His 254. These findings can be rationalized if the inhibitors, in particular TACA, mimic the transition state rather than the initial Michaelis–Menten complex. The proposed mechanism for GOX (Lindqvist & Brändén, 1989) involves an initial binding to Tyr 24, Arg 164, and Arg 257. These initial interactions are followed by the formation of the planar transition state in which additional interactions to His 254 and Tyr 129 are present.

The binding of the inhibitors presented here can thus be correlated to the proposed binding of substrate and the structure of the transition state. However, the unresolved question of the mechanism of initial proton abstraction cannot be resolved by the structures of the GOX inhibitor complexes presented here; neither of the proton transfer mechanisms can be excluded.

One surprising feature of the inhibitor complexes is the tilt of the isoalloxazine ring toward Thr 78. In the holoenzyme this residue is connected to O4 of FMN via a solvent molecule at the *re*-face of FMN. The position of the isoalloxazine ring in the enzyme-inhibitor complexes leaves no room for this water molecule. Thus, in the active site, a rearrangement of the flavin ring takes place upon binding of the inhibitors. In the reoxidation of FMN in the second half-reaction of the enzyme, the O4 atom of FMN was proposed to be bound in this pocket (Lindqvist & Brändén, 1989) for attack of oxygen on the *si*-face, which is in agreement with these inhibitor-complex structures.

Materials and methods

The inhibitors 4-Carboxy-5-(1-pentyl)hexylsulfanyl-1,2,3-triazole (TACA) and 3-Decyl-2,5-dioxo-4-hydroxy-3-pyrroline (TKP) were a gift from Zeneca Agrochemicals. The synthesis of TKP has been described previously (Rooney et al., 1983); TACA was designed and synthesized at Zeneca Agrochemicals Ltd (Viner et al., in prep.). The structure of the inhibitors and of the substrate glycolate are shown in Figure 1. Spinach glycolate oxidase was expressed and purified from *E. coli* as described by Macheroux et al. (1992) and Stenberg and Lindqvist (1996). Enzymatic activity was measured as described by Macheroux et al. (1991).

Crystallization

Wild-type GOX was mixed with 50 mM Tris–0.25 mg/mL FMN solution saturated with the inhibitor. For TKP, 0.5% JF5969 was also present to increase the solubility of the inhibitor. JF5969 has been shown not to inhibit GOX in a concentration of up to 4% (data not shown). The enzyme-inhibitor solutions were diluted until the GOX concentration was approximately 0.5 mg/mL and checked for activity. Excess undissolved inhibitor was removed from the sample by centrifugation and the samples were concentrated to a protein concentration of 20 mg/mL. Crystallizations were then set up using microcapillaries as previously described (Lindqvist & Brändén, 1979), with tertiary-butanol as precipitating agent and the mother liquor saturated with inhibitor, and with 0.5% JF5969 present for the TKP complex.

Crystallographic data collection

Crystallographic data for the TACA complex were collected at 4 °C on an R-AXIS IIc image plate on a Rigaku rotating anode, with crystal to detector distance set to 100 mm. Data for the TKP complex were collected on a MAR image plate at 4 °C with a crystal to detector distance of 150 mm. Data frames were collected as 1° oscillations in both cases. Data evaluation was performed using the program DENZO (Otwinowski, 1993). All further data processing was performed using the CCP4 program suite (1994). Data collection statistics are summarized in Table 1.

Model building and refinement

TACA-complex

Water molecules in the active site of the holoenzyme (Lindqvist, 1989; Protein Data Bank ID 1gox.pdb) were removed and a difference Fourier map using this model was calculated. The inhibitor was modeled into the positive electron density observed in the active site. 20005 unique reflections in the interval 8–2.6 Å were used in the refinement. In order to monitor progress of the refinement, a test set of 8% of the reflections was excluded for the calculation of R_{free}. The structure was refined using XPLOR (Brünger et al., 1987) using the Engh and Huber (1991) parameters. Parameters for the inhibitor were obtained from idealized coordinates using XPLO2D (Kleywegt, 1995). Cycles of positional refinement and rebuilding using the graphics program O (Jones et al., 1991) were performed. Finally temperature factors were refined. Despite the medium resolution (2.6 Å) individual B-factor refinement decreased R_{free} more than grouped B-factor refinement. The refinement statistics are summarized in Table 1.

TKP-complex

The coordinates of native GOX without bound water molecules were used as a search model to solve the structure using molecular replacement with the programs Rotfun and Trafun in the CCP4 package (1994).

In the first step, the rotation function, sampled every 2.5°, was calculated in the resolution range 20–3 Å. Only one significant solution was found with Euler angles 4.83°, 95.77°, and 254.81°. Translation–function calculations using this solution gave one peak corresponding to a translation of 4.83, 95.77, and 254.81 Å, with

correlation coefficient 57.2. After rigid body refinement a difference Fourier map was calculated and the inhibitor was modeled into the observed positive electron density present in the active site using O (Jones et al., 1991). Water molecules were incorporated using the programs Peakmax in the CCP4-suite (1994) and Peakcheck (J. Smith, unpubl.). The proposed water molecules were checked against the electron density map at 1.3σ contour level, and only the ones with clear density were incorporated into the model. Refinement was performed using 21198 individual reflections in the resolution interval 8–2.2 Å, with 8% of the data excluded for calculation of R_{free}. Several cycles of positional refinement and rebuilding using XPLOR (Brünger et al., 1987) and O (Jones et al., 1991) were conducted, and individual B-factors were refined. Refinement was ended when R_{free} stopped decreasing. The results of the refinement are summarized in Table 1. The parameters used were from Engh and Huber (1991), and the parameters for an idealized inhibitor were obtained using XPLO2D (Kleywegt, 1995).

Comparison of the two inhibitor complexes to the native structure was made using the option Lsq in the graphics program O (Jones et al., 1991). Atoms were considered to be structurally equivalent if they are within 3.2 Å and within a continuous stretch of minimum 5 equivalent atoms.

Acknowledgments

K.S. was supported by Zeneca Agrochemicals Ltd. and a grant from the Nordic program for energy research, and Y.L. by a grant from the Swedish Agricultural Research Council.

References

Brünger A, Kuriyan J, Karplus M. 1987. Crystallographic *R* factor refinement by molecular dynamics. *Science 235*:458–460.

CCP4. 1994. Collaborative Computational Project Number 4. The CCP4 suite: Programs for protein crystallography. *Acta Crystallogr D50*:760–763.

Engh RA, Huber R. 1991. Accurate bond angle parameters for X-ray protein structure refinement. *Acta Crystallogr A47*:392–400.

Fendrich G, Ghisla S. 1982. Studies on glycollate oxidase from pea leaves. Determination of stereospecificity and mode of inhibition by α-hydroxybutynoate. *Biochim Biophys Acta 30*:242–248.

Ghisla S, Massey V. 1989. Mechanisms of flavoprotein-catalyzed reactions. *Eur J Biochem 2*:243–289.

Jayanthi S, Saravanan N, Varalakkshmi P. 1994. Effect of DL α-lipoic acid in glyoxylate-induced acute lithiasis. *Pharmacol Res 30*:281–288.

Jones TA, Zou JY, Cowan SW, Kjeldgaard M. 1991. Improved methods for building protein models in electron density maps and the location of errors in these models. *Acta Crystallogr A 47*:110–119.

Kleywegt GJ. 1995. Dictionaries for heteros. *CCP4/ESF-EACBM Newsletter on Protein Crystallography 31*:45–50.

Kraulis PJ. 1991. MOLSCRIPT: A program to produce both detailed and schematic plots of protein structure. *J Appl Crystallogr 24*:946–950.

Lê KHD, Lederer F. 1991. Amino acid sequence of long chain α-hydroxy acid oxidase from rat kidney, a member of the family of FMN-dependent α-hydroxy acid-oxidizing enzymes. *J Biol Chem 266*:20877–20881.

Lederer F, Belmouden A, Gondry M. 1996. The chemical mechanism of flavoprotein-catalysed α-hydroxy acid dehydrogenation: A mutational analysis. *Biochem Soc Trans 24*:77–83.

Lindqvist Y, Brändén C-I. 1979. Preliminary crystallographic data for glycolate oxidase from spinach. *J Biol Chem 254*:7403–7404.

Lindqvist Y. 1989. Refined structure of spinach glycolate oxidase at 2 Å resolution. *J Mol Biol 209*:151–166.

Lindqvist Y, Brändén C-I. 1989. The active site of spinach glycolate oxidase. *J Biol Chem 264*:3624–3628.

Lindqvist Y, Brändén C-I, Mathews FS, Lederer F. 1991. Spinach glycolate oxidase and yeast flavocytochrome b_2 are structurally homologous and evolutionary related enzymes with distinctly different function and flavin mononucleotide binding. *J Biol Chem 266*:3198–3207.

Macheroux P, Massey V, Thiele DJ. 1991. Expression of spinach glycolate oxidase in *Saccharomyces cerevisiae*: Purification and characterization. *Biochemistry 30*:4612–4619.

Macheroux P, Mulrooney S, Williams CH Jr, Massey V. 1992. Direct expression of active spinach glycolate oxidase in *Escherichia coli*. *Biochim Biophys Acta 1132*:11–16.

Macheroux P, Kieweg V, Massey V, Söderlind E, Stenberg K, Lindqvist Y. 1993. Role of tyrosine 129 in the active site of spinach glycolate oxidase. *Eur J Biochem 213*:1047–1054.

Otwinowski Z. 1993. DENZO. In: Sawyer L, Isaac N, Bailey S, eds. *Data collection and processing*. SERC Daresbury Laboratory, Warrington, UK. pp 80–86.

Reid GA, White S, Black MT, Lederer F, Mathews FS, Chapman SK. 1988. Probing the active site of flavocytochrome b_2 by site-directed mutagenesis. *Eur J Biochem 178*:329–333.

Rooney CS, Randall WC, Streeter KB, Ziegler C, Cragoe EJ Jr, Schwam H, Michelson SR, Williams HWR, Eichler E, Duggan DE, Ulm EH, Noll RM. 1983. Inhibitors of glycolic acid oxidase. 4-Substituted 3-hydroxy-1H-pyrrole-2,5-dione derivatives. *J Med Chem 26*:700-714.

Stenberg K, Clausen T, Lindqvist Y, Macheroux P. 1995. Involvement of tyr24 and trp108 in substrate binding and substrate specificity of glycolate oxidase. *Eur J Biochem 228*:408–416.

Stenberg K, Lindqvist Y. 1996. High level expression, purification and crystallization of recombinant spinach glycolate oxidase in *Escherichia coli*. *Prot Expr Purif 8*:295–298.

Urban P, Lederer F. 1985. Intermolecular hydrogen transfer catalyzed by a flavodehydrogenase, bakers' yeast flavocytochrome b_2. *J Biol Chem 260*: 11115–11122.

Williams HWR, Eichler E, Randall WC, Rooney CS, Cragoe EJ, Streeter KB, Schwam H, Michelson SR, Patchett AA, Taub D. 1983. Inhibitors of glycolic acid oxidase. 4-Substituted 2,4-dioxobutanoic acid derivatives. *J Med Chem 26*:1196–1200.